Journal of Power Sources 203 (2012) 282–287

Contents lists available at SciVerse ScienceDirect

Journal of Power Sources

journal homepage: www.elsevier.com/locate/jpowsour

Preparation of poly(acrylic acid)/gelatin/polyaniline gel-electrolyte and its application in quasi-solid-state dye-sensitized solar cells

Ziying Tang, Jihuai Wu*, Qin Liu, Min Zheng, Qunwei Tang, Zhang Lan, Jianming Lin

Engineering Research Center of Environment-Friendly Functional Materials, Ministry of Education, Institute of Materials Physical Chemistry, Huaqiao University, Quanzhou 362021, China

ARTICLE INFO

Article history:
Received 18 July 2011
Received in revised form
14 November 2011
Accepted 15 November 2011
Available online 23 November 2011

Keywords:
Poly (acrylic acid)
Gelatin
Polyaniline
Gel-electrolyte
Quasi-solid-state dye-sensitized solar cells

ABSTRACT

A microporous hybrid polymer of poly(acrylic acid)/gelatin/polyaniline (PAA/Gel/PANI) is synthesized with a two-steps solution polymerization. Using this hybrid as polymer host, a gel-electrolyte with a high liquid absorbency of 16.45 ($g\,g^{-1}$) and a high conductivity of 14.38 mS cm^{-1} is prepared, then a quasi-solid-state dye-sensitized solar cell (QS-DSSC) is assembled. The polymer host is characterized by scanning electron microscopy (SEM), the functional groups on the polymer are identified by Fourier transform infrared spectroscopy (FTIR) and the photovoltaic tests of the QS-DSSCs are carried out by measuring current–voltage (*I–V*) curves. The QS-DSSC with this hybrid gel-electrolyte achieves a light-to-electric energy conversion efficiency of 6.94%.

1. Introduction

As a consequence of dwindling resources, solar energy is expected to play a crucial role as a future energy source, dye-sensitized solar cell (DSSC) is a strong candidate for next-generation solar cell and a credible alternative to conventional solar cell [1,2]. Since the first prototype of a DSSC was reported in 1991 by O'Regan and Gratzel [3], it has aroused an intensive interest over the past decades due to its low cost and simple preparation procedure [2,3]. Based on liquid electrolytes, a DSSC has achieved a high light-to-electric conversion efficiency of 12% [1,4]. However, the potential problems caused by the liquid electrolytes, such as the leakage and volatilization of liquid, are considered as some of the critical factors limiting the long-term performance and practical use of the DSSCs [5–7]. Recently, many efforts have been done to replace liquid electrolyte with all-solid-state electrolyte [8–13], ionic liquid electrolyte [14–16] and quasi-solid-state gel-electrolyte [5,6,17–22]. Especially, the quasi-solid-state gel-electrolyte attracts a great attention due to its higher conductivity and excellent long-term stability.

The gel-electrolyte is consisted of a polymer host, a solvent and an ionic conductor. In most polymer gel electrolytes, the polymer content is low, usually less than 20%, and a significant amount of organic solvent is retained. The limitation of solvent leakage and volatilization is an important issue for preparing gel-electrolyte. As we know, poly(acrylic acid) (PAA) is a super-absorbent polymer with three-dimensional (3D) network and hydrophilic groups, it can absorb large amounts of liquid and the absorbed liquid is hard to be released even under some pressure [23–25]. However, pure PAA is not a good absorbent for conventional organic solvent used in liquid electrolytes [6], due to the hydrophilic functional group of carboxyl groups in PAA. In order to improve their absorbency of organic solvents, a modification of the carboxyl groups or an introduction of amphiphilic groups is necessary.

In our previous work, by modifying PAA with amphiphilic gelatin [26], poly(ethylene glycol) (PEG) [6], glycerin [27] etc., we have successfully synthesized some kinds of gel-electrolytes based on the modified superabsorbents and which showed excellent stability and absorbent ability for liquid electrolyte [6]. In continuation of our studies, a microporous superabsorbent of poly(acrylic acid)/gelatin (PAA/Gel) was synthesized, and then aniline monomer HCl solution was absorbed into the PAA/Gel network and in situ polymerized, thus a modified PAA/Gel/PANI hybrid polymer was obtained. Using the PAA/Gel/PANI hybrid polymer as host, a gel-electrolyte with a high absorbency of 16.45 ($g\,g^{-1}$) and a high conductivity of 14.38 mS cm^{-1} was prepared. The gel-electrolyte was used to assemble quasi-solid-state dye-sensitized solar cell (QS-DSSC), and an energy conversion efficiency of 6.94% was achieved.

* Corresponding author. Tel.: +86 595 22692229; fax: +86 595 22692229.
E-mail address: jhwu@hqu.edu.cn (J. Wu).

0378-7753/$ – see front matter © 2011 Elsevier B.V. All rights reserved.
doi:10.1016/j.jpowsour.2011.11.039

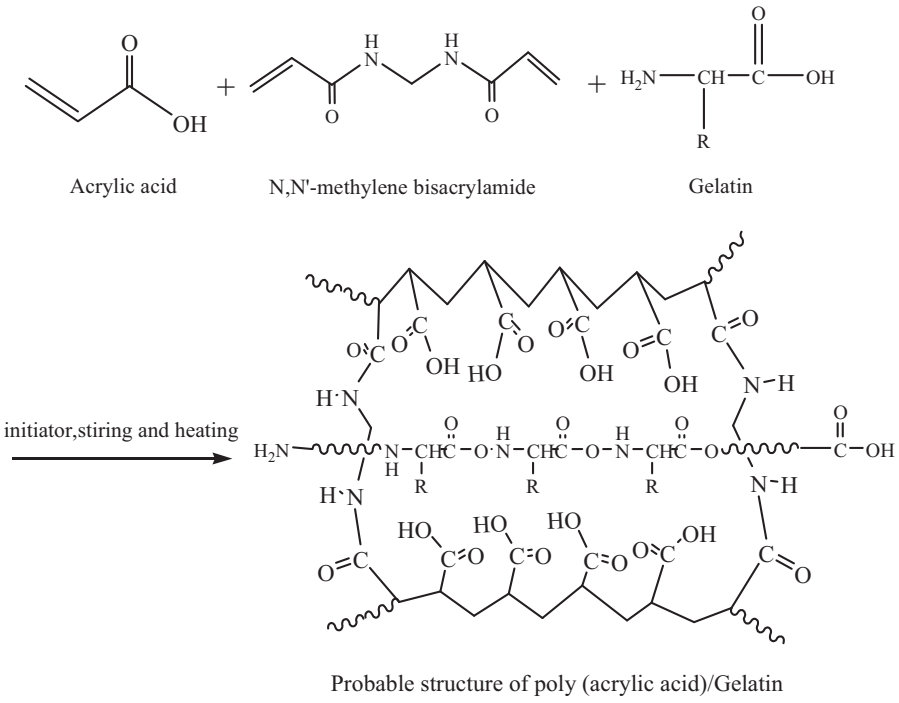

Fig. 1. The synthesis route of poly(acylic acid)/gelatin superabsorbent polymer.

2. Experimental

2.1. Materials

Acrylic acid monomer (AC), purchased from Shanghai Chemical Agent Company, China, was distilled under reduced pressure prior to use. The organometallic sensitized dye N-719 [$RuL_2(NCS)_2$, L = 4,4′-dicarboxylate-2,2′-bipyridine] was obtained from Solaronix SA (Switzerland). Titanium (IV) isopropoxide, poly(ethylene glycol) (molecular weight of 20,000 PEG-20000), gelatin, OP emulsification agent (Triton X-100) and other reagents were obtained from Shanghai Chemical Agent, China and used as received.

2.2. Synthesis of PAA/Gel superabsorbent polymer

PAA/Gel superabsorbent polymer was synthesized as follow by modifying the procedure from Refs. [6,26,28]: 1.0 g gelatin and 10 g acrylic acid monomer (AA) were dispersed in 15 ml distilled water. Subsequently, initiator potassium peroxydisulfate (KPS) (weight ratio of KPS to AA was 0.8%) and N,N′-methylene bisacrylamide (NMBA) (weight ratio of NMBA to AA was 0.05%) were added to the mixed solution system. Under a nitrogen atmosphere, a polymerization reaction took place under vigorous stirring at 80 °C. After the solution became viscous, the system was cooled to room temperature, then the resultant product was filtered and then washed in excess distilled water to remove any impurities. Finally, the product was vacuum dried at 80 °C for more than 12 h. Fig. 1 shows the synthesis of the PAA/Gel superabsorbent polymer.

2.3. Preparation of PAA/Gel/PANI hybrid polymer and gel-electrolyte

PAA/Gel/PANI hybrid polymer was prepared according to the following procedures [29,30]: 0.2 g of PAA/Gel was immersed in a predetermined amount of aniline (ANI) monomer and HCl solution (1 ml ANI, 300 ml H_2O, pH = 2.5) at ambient temperature for more than 48 h, which resulted in the absorption of ANI monomer into the PAA/Gel network and leaded to the formation of a swollen sample. After that, the swollen sample was soaked again in a KPS solution of 20 ml containing 0.0365 M KPS initiator, the polymerization reaction took place at 4 °C for more than 48 h in dark. When the swollen sample changed from original pale yellow color to dark green color, the conductive PANI polymer chain was in situ polymerized inside of the PAA/Gel network. After the polymerization process, similar to the preparation of PAA/Gel, the intermediate product was filtrated, washed, dried, thus a conductive PAA/Gel/PANI hybrid superabsorbent was obtained. Fig. 2 shows the possible structure of PAA/Gel/PANI polymer.

A gel-electrolyte was prepared by soaking 0.2 g dried PAA/Gel/PANI polymer in liquid electrolyte for more than 96 h to reach absorption saturation. The liquid electrolyte consisted of 0.1 M tetrabutylammonium iodide (TBAI), 0.1 M tetramethylammonium iodide (TMAI), 0.1 M tetraethylammonium iodide (TEAI), 0.1 M KI, 0.1 M LiI, 0.1 M NaI, 0.06 M I_2 in mixed organic solvent of N-methyl-2-pyrrolidone (NMP) and acetonitrile (AC) (NMP/AC = 2/8).

2.4. The assembling of DSSCs

A 10-μm-thick film of TiO_2 nanocrystals anode films was prepared by using a “doctor blade method”. A QS-DSSC with PAA/Gel or PAA/Gel/PANI based gel-electrolyte was fabricated by sandwiching a slice of gel-electrolytes between dye-sensitized TiO_2 anode

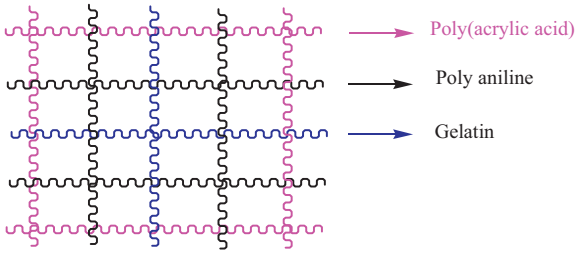

Fig. 2. Schematic structure of PAA/Gel/PANI hybrid superabsorbent.

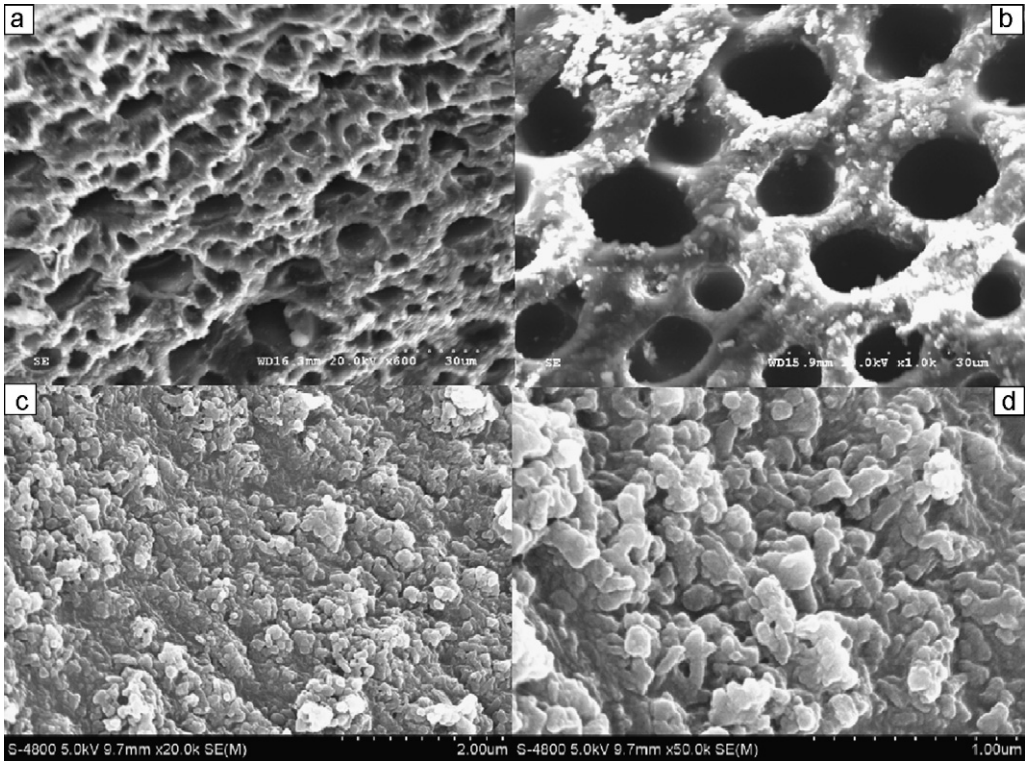

Fig. 3. SEMs of PAA/Gel/PANI superabsorbent polymer: (a, b) are the low magnification of polymer, (c, d) are the high magnification of polymer chain.

electrode and a platinum counter electrode. The detailed fabrication procedure for the nanocrystalline TiO_2 photoanodes and the assembly of DSSCs have been described by us elsewhere [6,31,32].

2.5. Characterizations

The morphology of PAA/Gel and PAA/Gel/PANI samples were studied by using a scanning electron microscope (SEM, Hitachi S-5200, Japan). The PAA/Gel or PAA/Gel/PANI sample was freeze dried by a freeze dryer (FD-1A-50, Beijing Boyikang Laboratory Instruments Co., Ltd, Beijing, China) then cut into a slice and coated with gold, and its surface was observed and photographed by SEM. The groups of PAA/Gel or other powdered samples were identified by Fourier transform infrared (FTIR) spectroscopy on a Nicolet Impact 410 FTIR spectrophotometer (Inspiratech 2000 Ltd., Warwickshire, UK) using KBr pellets.

2.6. Measurement

The liquid absorbency ($g\,g^{-1}$) of sample was measured according to the equation below [33]:

$$\text{Liquid absorbency} = \frac{W_2 - W_1}{W_1} \quad (1)$$

where W_1 is the mass of dried sample (g), W_2 is the mass of swollen gel-electrolyte (g). The ionic conductivity of gel-electrolyte was measured by using model DDSJ-308 digitized conductivity meter (Shanghai Reici Instrument Factory, China). The instrument was calibrated with 0.01 M KCl aqueous solution prior to experiments [6].

2.7. Photovoltaic test

The photovoltaic test of DSSC was carried out by measuring the *J–V* characteristic curves under a simulated solar illumination of 100 mW cm^{-2} (AM 1.5) from a 100 W xenon arc lamp (XQ-500 W, Shanghai Photoelectricity Device Company, China) in ambient atmosphere. The fill factor (*FF*) and light-to-electric energy conversion efficiency (η) of the cell were calculated according to the following equations [6]:

$$FF = \frac{V_{max} \times J_{max}}{V_{oc} \times J_{sc}} \quad (2)$$

$$\eta\ (\%) = \frac{V_{max} \times J_{max}}{P_{in}} \times 100\% = \frac{V_{oc} \times J_{sc} \times FF}{P_{in}} \times 100\% \quad (3)$$

where J_{sc} is the short-circuit current density (mA cm^{-2}), V_{oc} is the open-circuit voltage (V), P_{in} is the incident light power, and J_{max} (mA cm^{-2}) and V_{max} (V) are the current density and voltage in the *J–V* curves at the point of maximum power output, respectively.

3. Results and discussion

3.1. The morphology of PAA/Gel/PANI polymers

The SEM images PAA/Gel/PANI polymer were measured and shown in Fig. 3. From Fig. 3(a) and (b), it can be seen that the PAA/Gel/PANI shows a microporous network structure, owing to this structure and hydrophilic group on it, a large amount of organic solvent can be absorbed, and the absorbed organic solvent is hardly removed even under some pressure or heat, which is just the unique property of superabsorbent polymer [23,27]. Fig. 3(c) and (d) shows high magnification images of PAA/Gel/PANI polymer chain, from which we can see that the surface of PAA/Gel/PANI polymer is rough, and some ball-like or rod-like particles can be seen, the ball-like or rod-like particles is probably the in situ polymerized PANI particles. As mentioned above, when the ANI monomer was absorbed into the PAA/Gel network and in situ polymerized in the network during the second polymerization process, PANI chains are formed inside of the PAA/Gel network. As shown in Fig. 1, Because of the large amounts of O–H group on PANI molecule and the –COOH group on PAA and gelatin molecule, the PANI molecule can

Table 1
Liquid electrolyte absorbency and conductivity (σ) of the superabsorbents.

Superabsorbents	σ (mS cm^{-1}) (20 °C)	Liquid electrolyte absorbency (g g^{-1})
PAA/Gel	11.21	17.26
PAA/Gel/PANI	14.38	16.45
PAA/PEG[a]	6.12	<1.0
PAA/Gel/PPy[b]	14.10	–
PAA/PGA/PPy[c]	12.83	8.5

[a] From Ref. [6].
[b] From Ref. [26].
[c] From Ref. [27].

stably exist inside of PAA/Gel polymer with the existence of hydrogen bonds drive force, thus, an modified conductive PAA/Gel/PANI hybrid superabsorbent polymer generated ultimately.

3.2. Liquid absorbency and conductivity of PAA/Gel and PAA/Gel/PANI polymers

The liquid electrolyte absorbency capability and conductivity properties of PAA/Gel, PAA/Gel/PANI polymers were measured and listed in Table 1, the data for PAA/PEG, PAA/Gel/Ppy and PAA/PGA/PPy polymers previously reported [6,26,27] also added in Table 1. From the table, it can be seen that the liquid absorbency (g g^{-1}) of PAA/Gel and PAA/Gel/PANI was measured as 17.26 and 16.45 (g g^{-1}) respectively, which is higher than other polymer hosts [6,27]. Besides, the PAA/Gel can absorb more liquid electrolyte than the PAA/Gel/PANI, the less absorbency may arise from the introduction of PANI molecule inside of the polymer network, which results in a larger crosslinking density of the composite and leads to a decreased liquid absorbency [34]. On the other hand, PAA/Gel has a ANI solution absorbency of 9.62 g g^{-1}, the high adsorption of ANI solution ensures the high PANI amount inside of PAA/Gel polymer and benefits for the conductivity of polymer host.

Using the PAA/Gel and PAA/Gel/PANI as polymer host to prepare gel-electrolytes used in DSSCs, owing to the large amounts of liquid electrolyte absorbed in the gel-electrolyte, the ionic mobility and the connection between gel-electrolyte and TiO_2 film is improved, which benefits the photovoltaic performance of the DSSCs. From Table 1, the conductivity (σ) of PAA/Gel and PAA/Gel/PANI are 11.21 and 14.38 mS cm^{-1} respectively, and the best result is higher than the previously published reports [6,26,27]. Though the liquid absorbency of PAA/Gel is a little higher than that of PAA/Gel/PANI, the conductivity of PAA/Gel/PANI electrolyte is higher the PAA/Gel electrolyte because the introduction of the conductive PANI polymer chains inside of the polymer adds an electron transport channel, which leads to the electron transports more easily. It can be expected that the DSSC based on PAA/Gel/PANI hybrid superabsorbent can obtain an improved photovoltaic performance.

3.3. FTIR spectra of samples

Fig. 4 shows the FTIR spectroscopy of PAA/Gel (a), PANI (b), PAA/Gel/PANI (c). A middle strong and broad absorption band at 3300–3100 cm^{-1} was shown in curve (a), which arises from O–H and N–H stretching modes in PAA/Gel polymer, and the peeks at 1250 and 918 cm^{-1} are attributed to the O–H wagging vibration and C–N stretching vibration, respectively. The absorption peak at peak at 2960 cm^{-1} response for –CH_3, and the band centers at 1450, 1400, 800, 617 cm^{-1} arise from the –CH_2– wagging vibration, –CH_3 scissoring vibrations, C–H out-of-plane bending vibration, C–H out-of-plane deformation vibration, respectively. The characteristic peaks at 1720 cm^{-1} is responsible for C=O bending in COOH and the peak at 1170 cm^{-1} is due to C–O–C stretching vibration [27,33,35,36].

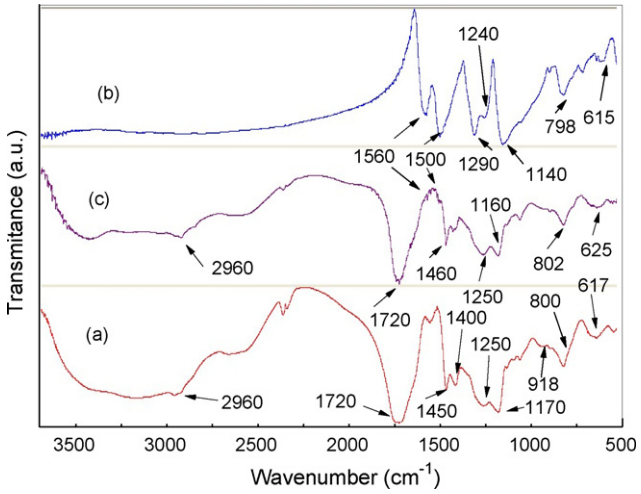

Fig. 4. FTIR spectra of PAA/Gel (a), PANI (b), PAA/Gel/PANI (c).

For PANI in curve (b), the characteristic peaks of PANI present near the wavenumbers of 1560, 1490 cm^{-1} ascribes from the stretching of quinoid and benzenoid, respectively. And the peeks around 1290 and 1240 cm^{-1} comes from the aromatic C–N and C–N$^+$ stretching vibration. The band centers at 1140, 798 and 615 cm^{-1} arise from C–H in-plane deformation, C–H out-of-plane bending vibration and C–H out-of-plane deformation vibration. These characteristic peaks in our work are account with the previous reports [37–42].

For PAA/Gel/PANI, curve (c) shows a similar FTIR spectrum as curve (a) except for some new peeks emerge in curve (c), such as the peaks at 1560, 1500 cm^{-1} responsible for C–C stretching mode for the quinoid ring and benzenoid in PANI. Besides, the C–H out-of-plane bending vibration at 802 cm^{-1}, and C–H out-of-plane deformation vibration at 625 cm^{-1} show a little red shift. Additionally, the peak at 1720 from C=O the –COOH bending split into two peaks, which may caused by the hydrogen bond interaction formed in the hybrid polymeric components after the in situ polymerization of PANI [17]. Summarily, the peak center changes indicate that the PANI is formed and stably exist inside of PAA/Gel polymer network.

3.4. Influence of temperature on the conductivity of gel-electrolyte

The conductivity–temperature (σ–T) relationships for the gel-electrolytes with PAA/Gel (a) and PAA/Gel/PANI (b) are shown in Fig. 5. From Fig. 5, it can be seen that the conductivity increased with the increase of temperature and the ln(σ) versus 1/T plots is almost linear, which is consist with the previous results [26,27,43]. The σ–T behavior for the gel-electrolytes based on PAA/Gel (a) and PAA/Gel/PANI (b) can be described by the Arrhenius equation shown as follow:

$$\ln\ \sigma = \ln A - \frac{E_a}{RT} \quad (4)$$

where σ is the conductivity, E_a is the activation energy, R is the molar gas constant, A is a meaningless constant, and T is absolute temperature. According to the experimental data, the E_a and A for the gel-electrolyte based on PAA/Gel/PANI are calculated as 8.69 kJ mol^{-1} and 507, and the E_a, A for the gel-electrolyte based on PAA/Gel is calculated as 10.13 kJ mol^{-1}, 772, respectively. Clearly, the gel-electrolyte with PAA/Gel/PANI has lower E_a and A than that with PAA/Gel, which indicates a faster transportation rate of I^-/I_3^- in PAA/Gel/PANI hybrid. In one word, the introduction of PANI to the polymer system has a positive effect on ionic

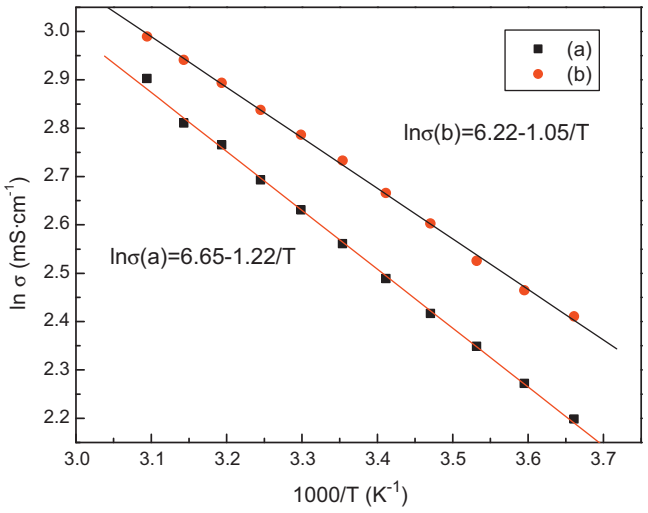

Fig. 5. Temperature dependence of the ionic conductivity (σ) for gel-electrolytes with PAA/Gel (a) and PAA/Gel/PANI (b) as polymer host.

conductivity of gel-electrolyte. In general, when an ionic transport process involves intermolecular ion hopping, the conductivity is determined by the thermal hopping frequency, which in turn is proportional to $\exp(-E_a/kT)$, and this leads to an Arrhenius conductivity–temperature relationship [6,27]. The ion hopping increases with an increase of temperature, which enhances the conductivity of the system.

3.5. Photovoltaic performance of DSSC

Under a simulated solar light irradiation of 100 mW cm^{-2} (AM 1.5), photocurrent–voltage curves of DSSCs with PAA/Gel (a) and PAA/Gel/PANI (b) gel-electrolytes were measured and shown in Fig. 6. The photoelectric parameters of DSSCs such as short circuit photocurrent density (J_{sc}), open circuit voltage (V_{oc}), fill factor (FF) and the overall energy conversion efficiency (η) are listed in Table 2. It is evident that all photovoltaic parameters of the DSSC with PAA/Gel/PANI gel-electrolyte are higher than that of the DSSC with PAA/Gel gel-electrolyte.

The η for the DSSC with PAA/Gel/PANI gel-electrolyte reaches 6.94%, while η for the DSSC with PAA/Gel gel-electrolyte is only 6.32%. The increased light-to-electric efficiency for the DSSC with

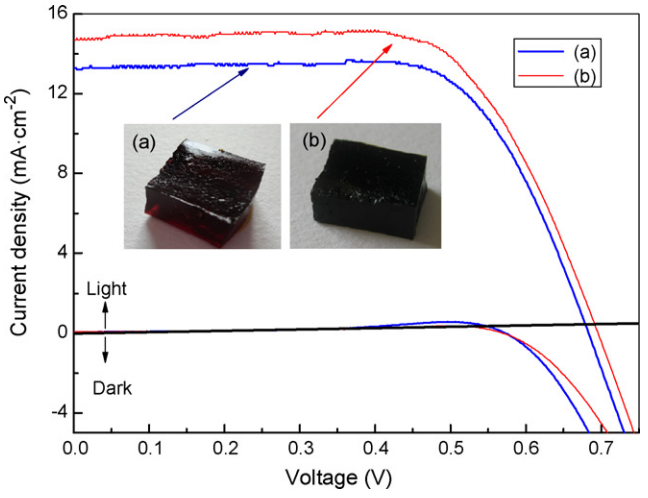

Fig. 6. Photocurrent–voltage curves of DSSCs with (a) PAA/Gel and (b) PAA/Gel/PANI gel-electrolytes (insert: digital photos of (a) and (b)).

Table 2
Photovoltaic performances of the DSSCs with PAA/Gel and PAA/Gel/PANI electrolytes.

Gel electrolyte	σ (mS cm^{-1})	J_{sc} (mA cm^{-2})	V_{oc} (V)	FF	η (%)
PAA/Gel	11.21	13.3	0.683	0.698	6.32
PAA/Gel/PANI	14.38	14.7	0.696	0.676	6.94

PAA/Gel/PANI attributes to the increased conductivity because of the introduction of PANI into the polymer network. As measured above, the introduction of PANI molecule leeds to a decreased E_a (from 10.13 to 8.69 kJ mol^{-1}) and a faster transportation rate of I^-/I_3^- in PAA/Gel/PANI hybrid polymer; besides, as our previous work [44], PANI has a good electrocatalytic activity for the I_3^-/I^- redox reaction, which causes a lower energy lose from I_3^- to I^-, the above two reasons result in an increased J_{sc} (from 13.3 to 14.7 mA cm^{-2}) and an enhanced η. In one word, the introduction of PANI into the gel-electrolyte is an efficient way to enhance the photovoltaic performance of the DSSCs.

Additionally, the dark current for the DSSC with PAA/Gel/PANI electrolyte is less than that for the DSSC with PAA/Gel electrolyte, which indicates a high utilization of I_3^- in the gel-electrolyte based on PAA/Gel/PANI hybrid polymer. As we know, the dark current is attributed to the I_3^- reduction by conduction band electrons at the semiconductor electrolyte junction (Eq. (5)) [45], in order to suppress the dark current reaction, it should decrease the connection between I_3^- and TiO_2 film and accelerate the reduction of I_3^- on Pt counter electrode.

$$I_3^- + 2e_{cb}^-(TiO_2) = 3I^- \quad (5)$$

As can be seen from the SEMs in Fig. 3, large amounts of microporous holes exist inside of PAA/Gel/PANI hybrid polymer host, it can deduce that when aniline monomer is absorbed into the PAA/Gel network, the polyaniline chain grows along the PAA/Gel polymer chain during the second polymerization process [30]. Because of that the PAA/Gel/PANI polymer host has an improved conductivity, the transportation rate of I^-/I_3^- is faster than that of PAA/Gel, so the I_3^- can be transported more fastly to the Pt-coated counter electrode and more efficiently reduced at the counter electrode instead of recombination with TiO_2 anode film. In other word, the PANI on PAA/Gel polymer host leads to a decreased dark current and a higher light-current.

The insert is the digital photos of PAA/Gel and PAA/Gel/PANI, from which it can see that the former seems dark red while the later completely changes to black. The color change of gel-electrolytes of PAA/Gel and PAA/Gel/PANI vividly proves the synthesis of modified PAA/Gel/PANI hybrid superabsorbent. The successful synthesis of superabsorbent based gel-electrolyte with high liquid absorbency and conductivity should accelerate the wide usage of DSSCs.

4. Conclusions

A PAA/Gel/PANI hybride modified superabsorbent was synthesized with two-steps solution polymerization. Using this polymer hybrid as host, a gel-electrolyte with an ionic conductivity of 14.38 mS cm^{-1} was obtained. By sandwiching the obtained gel-electrolyte between a dye sensitized TiO_2 electrode and a platinum counter electrode, a quasi-solid-state dye-sensitized solar cell with photocurrent density of 14.7 mA cm^{-2}, open circuit potential of 696 mV, fill factor of 0.676 and light-to-electric energy conversion of 6.94% was achieved. From the SEM observation, a large amounts of closed-microporous holes exist in PAA/Gel/PANI hybride polymer. The σ–T relationship and I–V test results show that the addition of PANI has a positive effect on the gel-electrolyte and the photovoltaic performance of the DSSC.

Acknowledgements

The authors thank for the joint support by the National High Technology Research and Development Program of China (No. 2009AA03Z217), the National Natural Science Foundation of China (Nos. 90922028, 50842027).

References

[1] M. Gratzel, Acc. Chem. Res. 42 (2009) 1788.
[2] M. Gratzel, Nature 414 (2001) 338.
[3] B. O'Regan, M. Gratzel, Nature 353 (1991) 737.
[4] Y.M. Cao, Y. Bai, Q.J. Yu, Y.M. Cheng, S. Liu, D. Shi, F.F. Gao, P. Wang, J. Phys. Chem. C 113 (2009) 6290.
[5] J.H. Wu, S. Hao, Z. Lan, J.M. Lin, M.L. Huang, Y.F. Huang, L.Q. Fang, S. Yin, T. Sato, Adv. Funct. Mater. 17 (2007) 2645.
[6] J.H. Wu, Z. Lan, J.M. Lin, M.L. Huang, S.C. Hao, T. Sato, S. Yin, Adv. Mater. 19 (2007) 4006.
[7] H.L. Lu, Y.H. Lee, S.T. Huang, C.C. Su, T.C.K. Yang, Sol. Energy Mater. Sol. Cells 95 (2011) 158.
[8] B. O'Regan, F. Lenzmann, R. Muis, J. Wienke, Chem. Mater. 14 (2002) 5023.
[9] P. Prene, E. Lancelle-Beltran, C. Boscher, P. Belleville, P. Buvat, C. Sanchez, Adv. Mater. 18 (2006) 2579.
[10] S.X. Tan, J. Zhai, M.X. Wan, Q.B. Meng, Y.L. Li, L. Jiang, D.B. Zhu, J. Phys. Chem. B 108 (2004) 18693.
[11] J.H. Wu, S. Hao, Z. Lan, J.M. Lin, M.L. Huang, Y.F. Huang, P.J. Li, S. Yin, T. Satot, J. Am. Ceram. Soc. 130 (2008) 11568.
[12] Q.B. Meng, K. Takahashi, X.T. Zhang, I. Sutanto, T.N. Rao, O. Sato, A. Fujishima, H. Watanabe, T. Nakamori, M. Uragami, Langmuir 19 (2003) 3572.
[13] P. Wang, Q. Dai, S.M. Zakeeruddin, M. Forsyth, D.R. MacFarlane, M. Gratzel, J. Am. Ceram. Soc. 126 (2004) 13590.
[14] P. Wang, S.M. Zakeeruddin, P. Comte, I. Exnar, M. Gratzel, J. Am. Ceram. Soc. 125 (2003) 1166.
[15] P. Wang, S. Zakeeruddin, J. Moser, M. Gratzel, J. Phys. Chem. B 107 (2003) 13280.
[16] P. Wang, S. Zakeeruddin, R. Humphry-Baker, M. Gratzel, Chem. Mater. 16 (2004) 2694.
[17] Z. Lan, J.H. Wu, S.C. Hao, J.M. Lin, M.L. Huang, Y.F. Huang, Energy Environ. Sci. 2 (2009) 524.
[18] R. Komiya, L.Y. Han, R. Yamanaka, A. Islam, T. Mitate, J. Photochem. Photobiol. A 164 (2004) 123.
[19] Z. Lan, J.H. Wu, J.M. Lin, M.L. Huang, J. Power Sources 164 (2007) 921.
[20] L.P. Stathatos, E. Zakeeruddin, S.M. Liska, P.M. Gratzel, Chem. Mater. 15 (2003) 1825.
[21] S. Agarwala, C.K.N. Peh, a.G.W. Ho, ACS Appl. Mater. Interfaces 3 (2011) 2383.
[22] P. Wang, S.M. Zakeeruddin, J.E. Moser, M.K. Nazeeruddin, T. Sekiguchi, M. Gratzel, Nat. Mater. 2 (2003) 498.
[23] J.H. Wu, J. Lin, M. Zhou, C. Wei, Macromol. Rapid Commun. 21 (2000) 1032.
[24] J.M. Lin, J.H. Wu, Z. Yang, M. Pu, Macromol. Rapid Commun. 22 (2001) 422.
[25] W.F. Lee, Y.C. Chen, Polym. Eur. J. 41 (2005) 1605.
[26] Q.H. Li, J.H. Wu, Z.Y. Tang, Y.M. Xiao, M.L. Huang, J.M. Lin, Electrochim. Acta 55 (2010) 2777.
[27] Z.Y. Tang, J.H. Wu, Q.H. Li, Z. Lan, L.G. Fan, J.M. Lin, M.L. Huang, Electrochim. Acta 55 (2010) 4883.
[28] Q.W. Tang, J.H. Wu, J.M. Lin, S.J. Fan, D. Hu, J. Mater. Res. 24 (2009) 1653.
[29] Q.W. Tang, J.H. Wu, H. Sun, J.M. Lin, S.J. Fan, D. Hu, Carbohydr. Polym. 74 (2008) 215.
[30] Q.W. Tang, J.M. Lin, J.H. Wu, C.J. Zhang, S.C. Hao, Carbohydr. Polym. 67 (2007) 332.
[31] J.H. Wu, Z. Lan, D.B. Wang, S.C. Hao, J.M. Lin, Y.L. Wei, S. Yin, T. Sato, J. Photochem. Photobiol. A 181 (2006) 333.
[32] J.H. Wu, Z. Lan, J.M. Lin, M.L. Huang, P.J. Li, J. Power Sources 173 (2007) 585.
[33] T.K. Mudiyanselage, D.C. Neckers, Soft Matter 4 (2008) 768.
[34] S. Wang, M. Yaszemski, J. Gruetzmacher, L. Lu, Polymer 49 (2008) 5692.
[35] Z.Y. Tang, X.Y. Wu, Z.S. Luo, Q.W. Tang, J.M. Lin, J.H. Wu, Polym. Adv. Technol. (2011), doi:10.1002/pat.1982.
[36] Q.W. Tang, J.H. Wu, Q.H. Li, J.M. Lin, Polymer 49 (2008) 5329.
[37] J. Tang, X. Jing, B. Wang, F. Wang, Synth. Met. 24 (1987) 231.
[38] R.N.A. David, M. Mohilner, W.J. Argersinger, J. Am. Ceram. Soc. 84 (1962) 3618.
[39] A. Zimmermann, U. Künzelmann, L. Dunsch, Synth. Met. 93 (1998) 17.
[40] Y. Sahin, K. Pekmez, A. Yildiz, Synth. Met. 129 (2002) 107.
[41] Q. Qin, J. Tao, Y. Yang, Synth. Met. 160 (2010) 1167.
[42] M. Zhao, X.M. Wu, C.X. Cai, J. Phys. Chem. C 113 (2009) 4987.
[43] Z. Lan, J. Wu, D. Wang, S. Hao, J. Lin, Y. Huang, Sol. Energy 80 (2006) 1483.
[44] Q.H. Li, J.H. Wu, Q.W. Tang, Z. Lan, P.J. Li, J.M. Lin, L.Q. Fan, Electrochem. Commun. 10 (2008) 1299.
[45] J.J. He, G. Benko, F. Korodi, T. Polivka, R. Lomoth, B. Akermark, L.C. Sun, A. Hagfeldt, V. Sundstrom, J. Am. Ceram. Soc. 124 (2002) 4922.